Journal of Alloys and Compounds 509 (2011) 7886–7890

Contents lists available at ScienceDirect

Journal of Alloys and Compounds

journal homepage: www.elsevier.com/locate/jallcom

Exchange biasing in SFMO/SFWO double perovskite multilayer thin films

Deepak Kumar, Davinder Kaur*

Functional Nanomaterials Research Laboratory, Department of Physics and centre of nanotechnology, IIT Roorkee, Roorkee 247667, Uttarakhand, India

ARTICLE INFO

Article history:
Received 24 August 2010
Received in revised form 2 May 2011
Accepted 3 May 2011
Available online 10 May 2011

Keywords:
Multilayer
SQUID
Exchange bias
Microstructure
Blocking temperature

ABSTRACT

In the present study, we have studied the exchange bias interaction in ferromagnetic Sr_2FeMoO_6 (SFMO)/antiferromagnetic Sr_2FeWO_6 (SFWO) multilayer thin films deposited on single crystal $LaAlO_3$ substrates using KrF pulsed laser deposition technique. XRD pattern revealed that SFMO, SFWO and their multilayer thin films were highly oriented along the *c*-axis. The microstructure studied by atomic force microscopy was found to be uniform, fine, dense and homogenous in nature. The observed magnetization-temperature curves showed Neel temperature $T_N \sim 37$ K for SFWO and Curie temperature $T_C > 320$ K for SFMO thin films. For multilayer, the field cooled magnetization–field curve was shifted horizontally and the direction of the horizontal shift is opposite to that of H_{FC}, indicating an exchange bias effect. Exchange bias field H_E was found to decrease with increase in temperature and approached to zero at blocking temperature.

1. Introduction

Exchange bias effect between ferromagnetic (FM) and antiferromagnetic (AFM) material was discovered in 1956 by Meiklejohn and Bean [1]. Although there has been some research in exchange bias of nanoparticles in the last decades, the bulk of exchange bias research remained focused mainly on thin film systems [2,3]. When a FM/AFM multilayer thin film is cooled through the Neel temperature (T_N) of antiferromagnetic material (T_N less than T_C, the curie temperature of the ferromagnetic material), the hysteresis loop of FM is now shifted or biased away from the origin. This shift is known as the exchange field (H_E), can be several hundreds Oersted in size. Antiferromagnetic layers are an important component of hard disk read heads and of non-volatile magnetic random access memory elements, MRAM. The effect of exchange bias at the interface between an antiferromagnetic (AFM) and a ferromagnetic (FM) layer expresses itself as a unidirectional pinning or anisotropy of the magnetization of the ferromagnet, and is utilized to fix the magnetization in a magnetic reference layer in a spin-valve structure or a magnetic tunnel junction (MTJ), which consists of two ferromagnetic layers separated by a non-magnetic metal (spin-valve) or an insulator (MTJ) [4–12].

The ideal structure of double perovskite materials can be viewed as a regular arrangement of corner-sharing BO_6 and $B'O_6$ octahedra, alternating along the three direction of crystal, with A cation occupying the voids in between the octahedra. The crystal structure and physical properties of double perovskite oxides ($A_2BB'O_6$) depend considerably on the size and valences of A, B and B′ cations. For instance, in Sr_2FeMoO_6 compound, the localized and coupled Fe spins of the Fe–O–Mo–O–Fe network through Mo 4d conduction electrons, give rise to a metallic ferromagnetic ($T_C \sim 420$ K) ground state [13–16]. Interestingly in the same line Sr_2FeWO_6 is an anti-ferromagnetic (AFM) insulator with a low Neel temperature ($T_N \sim 37$ K) as Fe–O–W–O–Fe network enhances super-exchange coupling [17–19]. The origin of such a different behavior is mainly due to the 2p(O)–5d(W) orbital hybridization in Sr_2FeWO_6 compound, being stronger than the 2p(O)–4d(Mo) hybridization in Sr_2FeMoO_6 compound [20], which in turn pushes the 5d(W) band toward higher energies producing an insulating ground state and thereby inhibiting the ferromagnetic interaction active in Sr_2FeMoO_6 compound [21,22]. Both the FM SFMO and AFM SFWO compositions exhibit tetragonally distorted perovskite structure with lattice mismatch of about 0.8% and are chemically compatible. The small mismatch and the chemical compatibility between the FM and AFM layers allow the growth of epitaxial heterostructures with almost atomically perfect interfaces.

The main objective of the present study is to fabricate the high quality SFMO, SFWO and [SFMO (100 Å)/SFWO (40 Å)]$_{15}$ multilayer thin films and to examine the effect of temperature on exchange bias. To the best of our knowledge, there is no report on SFMO/SFWO multilayer thin films in literature. The values of the exchange field H_E and coercivity H_C, as a function of temperature, were measured and the blocking temperature was found.

2. Experimental

SFWO, SFMO and [SFMO (100 Å)/SFWO (40 Å)]$_{15}$ were fabricated on single crystalline $LaAlO_3$ substrate using multitarget pulsed laser deposition technique (Excel instruments, India). In order to synthesize the multilayer structure, SFMO and SFWO

* Corresponding author.
E-mail address: dkaurfph@iitr.ernet.in (D. Kaur).

0925-8388/$ – see front matter © 2011 Elsevier B.V. All rights reserved.
doi:10.1016/j.jallcom.2011.05.006

targets were mounted on a step-motor controlled rotable carrier which allowed different targets to be sequentially exposed to the beam paths. To ablate sintered pellet targets, a pulsed laser beam generated by a KrF excimer laser (Lambda Physik) at a wavelength of 248 nm and pulse duration of 25 ns was introduced into the deposition chamber through a quartz window and focused using an optical lens onto the target surface. No external field was applied during deposition. Before every deposition, the targets were pre-ablated for 1 min in order to ascertain the same state of the target in every deposition. For removing magnetic contamination, the $LaAlO_3$ substrates were cleaned sequentially with concentrated HCl solution and trichloro ethylene, and then rinsed with deionized water. The substrate size was taken $5 \times 5\ mm^2$ which is smaller than the confined plume of our PLD, ensuring that there is no thickness gradient across the sample. The thickness of the films was measured using surface profiler and was kept constant for SFWO and SFMO thin films at approx. 220 nm. In case of multilayer, first layer of SFWO (40 Å) was deposited on the substrate followed by SFMO (100 Å) layer. In the present work, fifteen such bi-layers were deposited so the total thickness of multilayer was approx. 210 nm.

The orientation & crystallinity of these films were investigated using Bruker AXS D-8 advanced diffractometer of Cu Kα (1.54 Å) in θ–2θ geometry. To obtain a profile fitting with good signal, polycrystalline silicon powder was used for instrumental correction. Atomic force microscopy (NT-MDT: NTEGRA Model) was used in contact mode to study the surface morphology of these films. The root-mean-square roughness (R_{rms}) and average roughness (R_{avg}) of the surface was calculated three times at a different spot for each sample by AFM scan over $(2 \times 2)\ \mu m^2$ scanning area. For the exchange bias study, samples were heated to temperature of 320 K and cooled down to 5 K in the field of 1 T applied parallel to film surface [23]. Magnetic properties of the samples were characterized using superconducting quantum interference device (quantum design) in an applied magnetic field of ±7 T.

3. Results and discussion

3.1. Structural properties

Fig. 1 shows the high angle X-ray diffraction pattern of SFWO, SFMO and $[SFMO/SFWO]_{15}$ multilayer thin film at room temperature deposited on $LaAlO_3$ substrate at fixed deposition temperature and pressure of 825 °C and 2×10^{-5} Torr, respectively. It was observed that all these films exhibit only diffraction peaks corresponding to (0 0 1) reflections and the substrate, suggesting that the films were highly oriented along the *c*-axis, perpendicular to the growth. A small reflection corresponding to (1 0 1) plane at $2\theta = 19.6°$ was also observed (inset of Fig. 1) depicting the ordering of Fe/Mo ions at the B/B′ sites in these films [24]. Therefore the films are textured [25]. The crystallite size of these films was calculated using Scherrer's formula and was found to be 10.1, 27.5 and 12.2 nm for SFWO, SFMO and $[SFMO/SFWO]_{15}$, respectively.

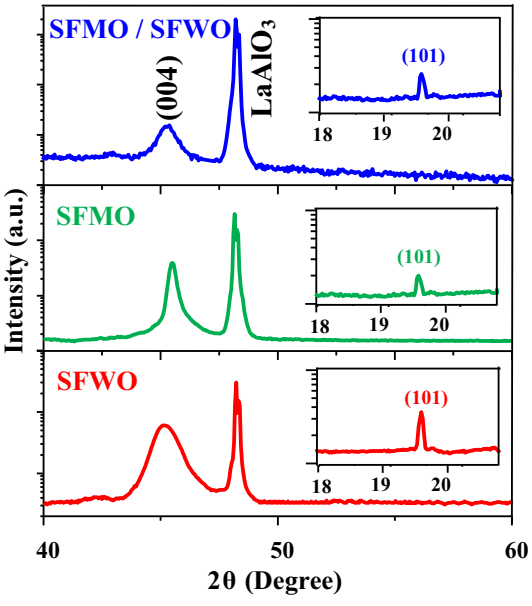

Fig. 1. High angle X-ray diffraction pattern of SFWO, SFMO and $[SFMO/SFWO]_{15}$ multilayer thin films. The inset shows the order-related diffraction peak of (1 0 1) plane.

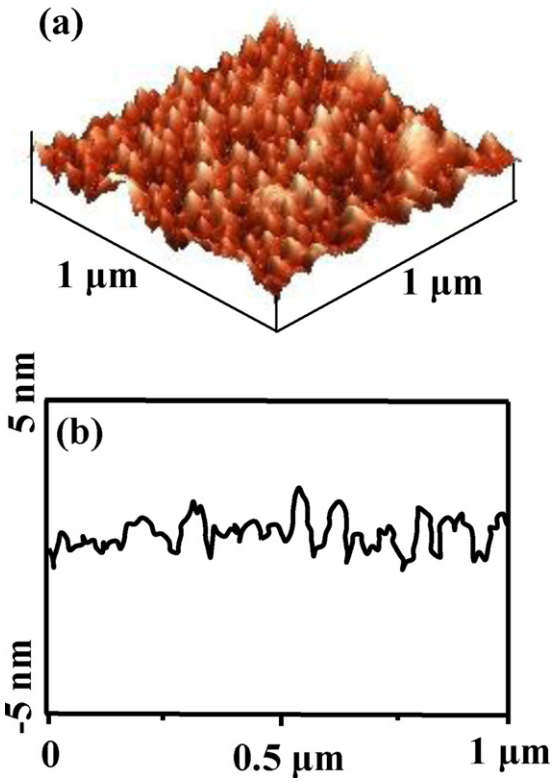

Fig. 2. Three-dimensional atomic force microscopy image and line scan of the surface of $[SFMO/SFWO]_{15}$. Scan was done over a 1 μm square area of the sample in contact mode.

Fig. 2 shows the 3D atomic force microscopy microstructure and line scan of the surface of multilayer thin film. The microstructure was found to be uniform, fine, dense and homogenous in nature. Atomic force microscopy was used to estimate the grain size, average roughness and root-mean-square roughness. The average roughness (R_{avg}) and root-mean-square roughness (R_{rms}) are defined from the following relationships: [26]

$$R_{avg} = \frac{1}{N}\sum_{i=1}^{N}\left|Z_i - \overline{Z}\right| \quad (1)$$

$$R_{avg} = \frac{1}{N}\left[\sum_{i=1}^{N}\left|Z_i - \overline{Z}\right|^2\right]^{1/2} \quad (2)$$

where N is the number of surface height data and $\overline{Z}$ the mean-height distance. The value of grain size, average roughness and root-mean-square roughness was found to be 19 nm, 1 nm and 1.4 nm, respectively.

The overall particle size shown by AFM was much bigger than that calculated by XRD, which is ascribed to the fact that AFM shows agglomeration of the particles whereas XRD gives an average mean crystallite size. The XRD and AFM data can be reconciled by the fact that smaller primary particles have a large surface free energy and would, therefore, tend to agglomerate faster and grow into larger grains.

3.2. Magnetic properties

Magnetic properties of these multilayers were measured using a SQUID magnetometer. The magnetization data for all the films

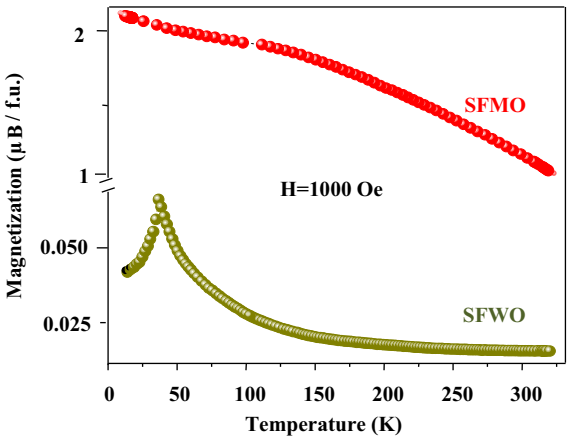

Fig. 3. Temperature dependence of field cooling (FC) average in-plane magnetization of SFWO and SFMO thin films measured at a constant magnetic field of 1000 Oe.

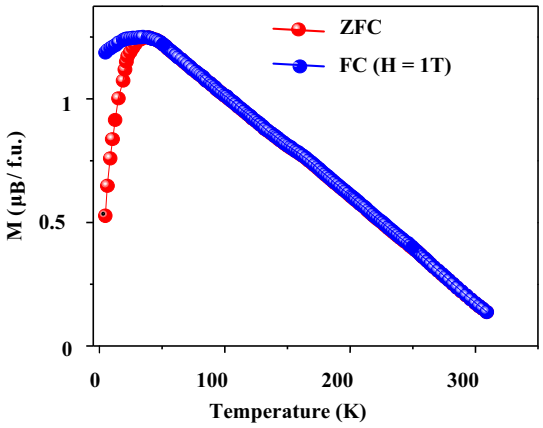

Fig. 4. Magnetization as a function of temperature for a $[SFMO/SFWO]_{15}$ multilayer thin film. The measurements were performed by warming up in 1 T after having cooled down to 5 K, in zero field (ZFC) and 1 T (FC), respectively.

was corrected to account for the diamagnetic contribution of the $LaAlO_3$ (0 0 1) substrate using equation

$$M_{film}(H) = M_{total}(H) - \chi_{substrate} \times H \quad (3)$$

where $\chi_{substrate}$ is the susceptibility of the substrate, M_{total} is the magnetization of sample (film + substrate) and H is the applied magnetic field which is parallel to film surface. The measured value of susceptibility for $LaAlO_3$ substrate is -3.09×10^{-8}. The temperature dependence of the field cooling (FC) average in-plane magnetization of SFWO and SFMO films are shown in Fig. 3. These curves were recorded by warming up in a measurement field of 1000 Oe after having cooled in the same field. In case of SFWO film, a cusp at 36.7 K was observed, which corresponds to antiferromagnetic transition temperature. On the other hand, FC curve of SFMO thin films showed the continuous decrease in magnetization with corresponding increase in temperature from 10 K to 320 K. No transition was observed in this temperature range which indicates that the curie temperature of SFMO thin film is higher than 320 K [27]. The temperature dependence of the zero-field cooling (ZFC) and field cooling (FC) average in-plane magnetization of $[SFMO/SFWO]_{15}$ multilayer film is shown in Fig. 4. Both curves were recorded by warming up in a measurement field of 1 T after having cooled in zero field and in the same field (H = 1 T), respectively. Note that below 30 K the FC and ZFC magnetization curves are split. The temperature above which the two curves overlap has been designated as the magnetic blocking temperature T_{BM} of the FM/AFM system [28].

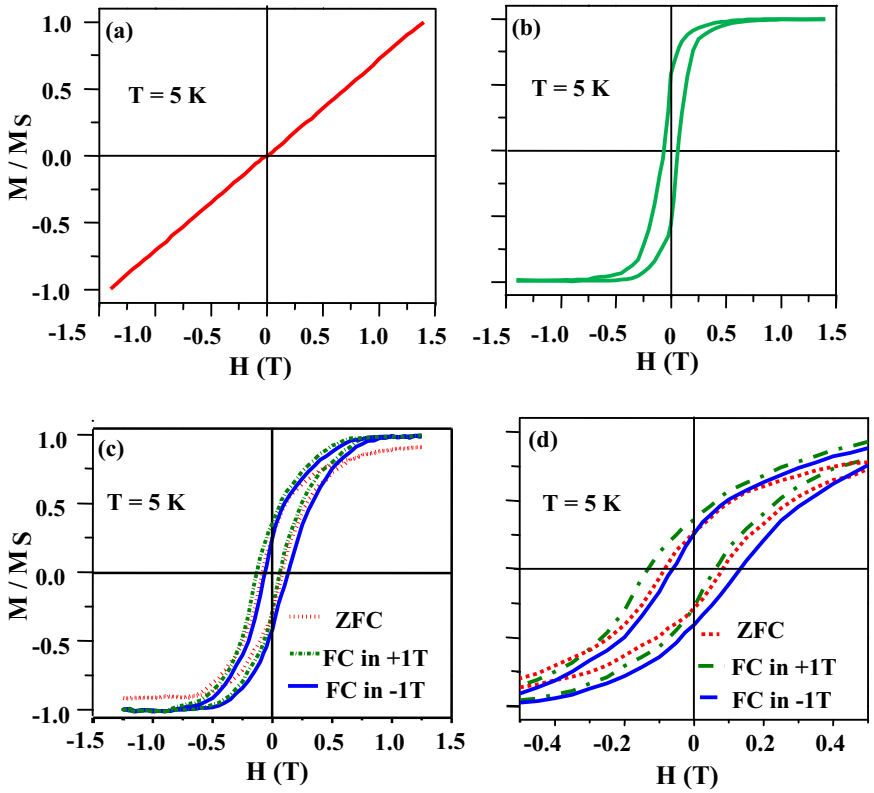

Fig. 5. Hysteresis loops, measured at 5 K after cooling down from 320 K in zero field cooled (ZFC) for (a) SFWO film, (b) SFMO film and (c) $[SFMO/SFWO]_{15}$ multilayer thin film along hysteresis loops for field cooled (FC) in ±1 T, (d) enlarge view of.

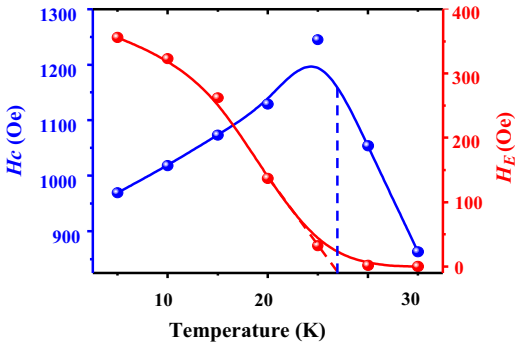

Fig. 6. Temperature dependence of the coercivity H_C and exchange bias field H_E for [SFMO (100 Å)/SFWO (40 Å)]$_{15}$ multilayer film. The vertical dashed line indicates the blocking temperature.

The M–H loop for SFMO and [SFMO/SFWO]$_{15}$, obtained after ZFC clearly exhibits hysteresis arising from ferromagnetic SFMO and is symmetric with respect to a 180° rotation around the origin, and for SFWO it shows antiferromagnetic behavior [Fig. 5(a)–(d)]. The shapes of M–H loops obtained at 5 K after FC ($H_{FC} = \pm 1$ T) remain same as the shape after the ZFC loop for SFWO and SFMO films while for multilayer, it shifts horizontally and the direction of the horizontal shift is opposite to that of H_{FC}, as in the case of various exchange bias systems. The two loops with FC at +1 T and −1 T fields in Fig. 5(d) are giving a clear evidence that the observed loop-shift is really exchange bias, not minor loop effect, because the loop always shifts toward the direction opposite the cooling field. Otherwise, if this is minor loop effect then it just shifts toward the right no matter which direction the FC is applied. This indicates that the exchange bias is caused by interaction between FM and AFM spins at the SFMO/SFWO interface. The exchange bias field H_E and coercivity H_C are calculated using

$$H_E = -\left(\frac{H_1 + H_2}{2}\right) \quad (4)$$

$$H_C = \left|\frac{H_1 - H_2}{2}\right| \quad (5)$$

where H_1 and H_2 denote the negative field and the positive field at which the magnetization becomes zero, respectively [29]. Thus, an exchange bias field $H_E \sim 0.036$ T and enhanced coercivity ($H_C = 0.084$ T in the ZFC case and $H_C = 0.097$ T in the FC one) are calculated from the hysteresis loop measurements at 5 K.

Fig. 6 shows variation of exchange bias field H_E and coercivity H_C as a function of temperature. Exchange bias field H_E decreases with increase in temperature and approaches to zero above 27 K (exchange bias blocking temperature, T_B). Note that $T_B \sim T_{BM}$. On the other hand, H_C initially increases with increase in temperature and then decreases after reaching a maximum value at around T_B. Similar peaks in H_C at T_B observed in oxidized NiFe layers have been explained using a thermal fluctuation model by Fulcomer and Charap [30]. They assumed that the small oxide particles were only coupled to the magnetic NiFe film but independent of each other. In this form, the varying sizes of particles would lead to superparamagnetism. In the present study, it is highly unlikely that the grains would behave independent of each other because of the dense, continuous nature of the films as shown in Fig. 2. A more recent mean-field theory by Wee et al. [31], which considers an epitaxial system, has shown similar results for uncompensated interfaces based on a parallel domain wall. They predict a blocking temperature that arises due to thermal dissipation of a domain wall, where T_B is the temperature at which the domain wall is no longer sustainable. Stiles and McMichael give a description of peaks in H_C which combines aspects of both the theories described above using a mesoscopic model assuming effective magnetic moments for the grains of the AF [32]. Generally, the important point is that in this temperatures range, a large fraction of the hysteretic losses occur in the AF layer, giving rise to an enhanced coercivity. The broad maxima in H_C occur only for the thicker ferromagnetic layers [33]. The interaction between the two layers still exists above T_B which can be seen from the significantly enhanced H_C. The true nature of this interaction is open for debate. In models such as those mentioned above, beyond T_B the entire spin structure of the AF layer reverses with the ferromagnet as the energy barrier holding it in place can be overcome by the torque exerted by the ferromagnetic spins once it has dropped below a certain height. However, one cannot exclude that an AF even in its paramagnetic phase has some influence on the reversal of the ferromagnet. The AF experiences an interfacial exchange field originating from the ferromagnet and a paramagnet in a field that has a magnetization. Naturally, it must follow the ferromagnet during reversal, which means that it is reversible, and will yield zero H_E but possibly an enhanced H_C. Leighton et al. have interpreted such an effect in terms of AF spin fluctuations at the surface of the AF layer inducing a uniaxial anisotropy in the interfacial region of the F layer which leads to a coercivity enhancement [34].

4. Conclusion

In summary, high-quality epitaxial SFWO, SFMO and [SFMO/SFWO]$_{15}$ multilayer thin films were fabricated using PLD on (0 0 1)-$LaAlO_3$ single-crystalline substrates. Exchange bias effect in SFMO/SFWO multilayers was systematically studied as a function of temperature. Hysteresis loop of the multilayer showed horizontal shift at 5 K, below the blocking temperature ($T_B \sim 27$ K). This result indicated that the exchange bias effect is caused by the interaction between FM and AFM spins at the interface. On the basis of dependence of the horizontal loop shift, an exchange-bias field $H_E = 0.036$ T and an enhanced coercive field $H_C = 0.097$ T were obtained at 5 K after cooling the sample in an external magnetic field of 1 T.

Acknowledgment

The financial support provided by Department of Information Technology (DIT), India under Nanotechnology Initiative Program with Reference Grant No. 20(11)/2007-VCND is highly acknowledged. The author Deepak Kumar is thankful to CSIR for award of senior research fellowship. The authors wish to thank Dr. Nguyen Nguyen Phuoc (Department of Physics, Center for Superconducting and Magnetic Materials, National University of Singapore) for enlightening discussion.

References

[1] W.H. Meiklejohn, C.P. Bean, Phys. Rev. 102 (1956) 1413.
[2] J. Nogues, I.K. Schuller, J. Magn. Magn. Mater. 192 (1999) 203.
[3] M. Kiwi, J. Magn. Magn. Mater. 234 (2001) 584.
[4] G.A. Prinz, Science 282 (1998) 1660.
[5] S.A. Wolf, D.D. Awschalom, R.A. Buhrman, J.M. Daughton, S. Von Molnar, M.L. Roukes, A.Y. Chtchelkanova, D.M. Treger, Science 294 (2001) 1488.
[6] B. Dieny, V.S. Speriosu, S.S.P. Parkin, B.A. Gurney, D.R. Wilhoit, D. Mauri, Phys. Rev. B 43 (1991) 1297.
[7] J.C.S. Kools, IEEE Trans. Magn. 32 (1996) 3165.
[8] Y. Wu, in: H.S. Nalwa (Ed.), Encyclopedia of Nanoscience and Nanotechnology, vol. 7, American Scientific Publishers, Stevenson Ranch, 2004, p. 493.
[9] J.F. Bobo, L. Gabillet, M. Bibes, J. Phys. Condens. Matter 16 (2004) S471.
[10] S.S.P. Parkin, Annu. Rev. Mater. Sci. 25 (1995) 357.
[11] B.N. Engel, N.D. Rizzo, J. Janesky, J.M. Slaughter, R. Dave, M. DeHerrera, M. Durlam, S. Tehrani, IEEE Trans. Nanotechnol. 1 (2002) 32.
[12] K.M.H. Lenssen, D.J. Adelerhof, H.J. Gassen, A.E.T. Kuiper, G.H.J. Somers, J.B.A.D. van Zon, Sens. Actuators A: Phys. 85 (2000) 1.
[13] K.I. Kobayashi, T. Kimura, H. Sawada, K. Terakura, Y. Tokura, Nature (London) 395 (1998) 677.
[14] A.S. Ogale, S.B. Ogale, R. Ramesh, T. Venkatesan, Appl. Phys. Lett. 75 (1999) 537.
[15] L. Balcels, J. Navarro, M. Bibes, A. Roig, B. Martinez, J. Fontcuberta, Appl. Phys. Lett. 78 (2001) 781.

[16] Y. Tomioka, T. Okuda, Y. Okimoto, R. Kumai, K.I. Kobayashi, Y. Tokura, Phys. Rev. B 61 (2000) 422.
[17] G. Blasse, Philips Res. Rep. 20 (1965) 327.
[18] T. Nakagawa, K. Yoshikawa, S. Nomura, J. Phys. Soc. Jpn. 27 (1999) 880.
[19] H. Kawanaka, I. Hase, S. Toyama, Y. Nishihara, J. Phys. Soc. Jpn. 68 (1999) 2890.
[20] Z. Fang, K. Terakura, J. Kanamori, Phys. Rev. B 63 (2001) 180407.
[21] D.D. Sarma, P. Mahadevan, T. Saha-Dasgupta, S. Ray, A. Kumar, Phys. Rev. Lett. 85 (2000) 2549.
[22] D.D. Sarma, Curr. Opin. Solid State Mater. Sci. 5 (2001) 261.
[23] N.N. Phuoc, T. Suzuki, J. Appl. Phys. 101 (2007) 09E501.
[24] D.D. Sarma, S. Ray, K. Tanaka, M. Kobayashi, A. Fujimori, P. Sanyal, H.R. Krishnamurthy, C. Dasgupta, Phys. Rev. Lett. 98 (2007) 157205.
[25] M.R. Fitzsimmons, C. Leighton, J. Nogues, A. Hoffmann, K. Liu, C.F. Majkrzak, J.A. Dura, J.R. Groves, R.W. Springer, P.N. Arendt, V. Leiner, H. Lauter, I.K. Schuller, Phys. Rev. B 65 (2002) 134436.
[26] H.S. Zhang, J.L. Endrino, A. Anders, Appl. Surf. Sci. 255 (2008) 2551.
[27] D. Kumar, D. Kaur, Physica B 405 (2010) 3259.
[28] V. Skumryev, S. Stoyanov, Y. Zhang, G. Hadjipanayis, D. Givord, J. Nogues, Nature (London) 423 (2003) 850.
[29] D. Magnoux, D. Hrabovsky, P. Baules, M.J. Casanove, E. Snoeck, A.R. Fert, J.F. Bobo, J. Appl. Phys. 91 (2002) 7730.
[30] (a) E. Fulcomer, S.H. Charap, J. Appl. Phys. 43 (1972) 4190;
(b) E. Fulcomer, S.H. Charap, J. Appl. Phys. 43 (1972) 4184.
[31] L. Wee, R.L. Stamps, R.E. Camley, J. Appl. Phys. 89 (2001) 6913.
[32] M. Stiles, R.D. Mc Micheal, Phys. Rev. B 63 (2001) 064405.
[33] C. Leighton, M.R. Fitzsimmons, A. Hoffmann, J. Dura, C.F. Majkrzak, M.S. Lund, I.K. Schuller, Phys. Rev. B 65 (2002) 064403.
[34] C. Leighton, H. Suhl, M.J. Pechan, R. Compton, J. Nogues, I.K. Schuller, J. Appl. Phys. 92 (2002) 1483.